Journal of Alloys and Compounds 499 (2010) 144–148

Contents lists available at ScienceDirect

Journal of Alloys and Compounds

journal homepage: www.elsevier.com/locate/jallcom

Towards $Y(NH_2BH_3)_3$: Probing hydrogen storage properties of YX_3/MNH_2BH_3 (X = F, Cl; M = Li, Na) and $YH_{x\sim3}/NH_3BH_3$ composites☆

Radostina V. Genova[a], Karol J. Fijalkowski[b], Armand Budzianowski[a], Wojciech Grochala[a,b,*]

[a] ICM, The University of Warsaw, Pawińskiego 5a, 02106 Warsaw, Poland
[b] Faculty of Chemistry, The University of Warsaw, Pasteura 1, 02093 Warsaw, Poland

ARTICLE INFO

Article history:
Received 29 December 2009
Received in revised form 13 March 2010
Accepted 21 March 2010
Available online 27 March 2010

Keywords:
Hydrogen storage materials
Amidoboranes
Yttrium

ABSTRACT

Alkali and alkaline-earth metal amidoboranes constitute a new class of inorganic hydrogen storage materials containing distinct $[NH_2BH_3]^-$ units. Here we have attempted synthesis of one of the lightest among M(III) amidoboranes, $Y(NH_2BH_3)_3$, with its high nominal hydrogen content of 8.4 wt.%, using few different routes. Polycrystalline $Y(NH_2BH_3)_3$, successfully obtained via mechanochemical synthesis utilizing $LiNH_2BH_3$ and YCl_3, has been subject to structural and spectroscopic investigations as well as studies of thermal decomposition. $Y(NH_2BH_3)_3$ crystallizes monoclinic ($C2/c$) with $a = 13.18902(63)$ Å, $b = 7.82233(38)$ Å, $c = 14.874274(68)$ Å, $\beta = 92.42620(40)^\circ$ ($Z = 8$, $V = 1533.19(13)$ Å^3). The title compound is quite unstable at ambient conditions and it spontaneously decomposes within several days. When heated up in argon, it exothermally emits hydrogen contaminated with significant amount of ammonia, in the 50–250 °C temperature range.

© 2010 Elsevier B.V. All rights reserved.

1. Introduction

Ammonia borane (AB, NH_3BH_3) contains ~19.6 wt.% of hydrogen [1] and as such it is an important hydrogen storage material [2]. The molecule of AB consists of hydridic B–H and protic N–H parts and a strong B–N bond that makes hydrogen evolution from solid more favorable than dissociation to ammonia (Lewis base) and diborane (Lewis acid). Interestingly, AB may serve itself as an acid in its reactions with strong ionic hydride Lewis bases (LiH [3–5], NaH [4,6], CaH_2 [5,7], and SrH_2 [8]) while forming metal amidoboranes.

Although amidoboranes of lithium [4,5], sodium [3,6], calcium [5,7], and strontium [8] have been obtained and characterized, yet, up to now the amidoboranes of trivalent elements have not been reported in the literature [9]. In the present work we focused on synthesis and characterization of $Y(NH_2BH_3)_3$ [10]. We were interested whether this compound could exhibit H_2 storage properties superior to amidoboranes of mono- and divalent cations. Theoretical hydrogen content of $Y(NH_2BH_3)_3$ is pretty large, some 8.4 wt.%.

We have attempted to synthesize $Y(NH_2BH_3)_3$ via five different 'dry' mechanochemical pathways. We avoided irreversible coordination of oxa-solvents (THF, Et_2O) to Y^{3+} using 'dry' mechanochemical synthesis (high-energy disc-milling). Only one reaction has yielded crystalline $Y(NH_2BH_3)_3$. The thermodynamically unstable product is similar to amidoboranes of other metals and it releases most of hydrogen stored in the temperature range of 50–250 °C.

2. Experimental

2.1. Dry synthesis

Operations with all substrates and products were performed inside a Labmaster DP MBRAUN glovebox under argon atmosphere ($O_2 < 1.0$ ppm; $H_2O < 0.1$ ppm). Exposure of samples to atmospheric oxygene and moisture was minimized.

We have used the highest purity commercially available NH_3BH_3 (98% JSC Aviabor). YH_{3-x} was synthesized from metallic yttrium (99.9% Sigma Aldrich) and hydrogen (99.999% Air Products) in the PCT Pro-2000 equipment (Hy-Energy LLC, USA) (20 bar, 300 °C, 162 h). A non-stoichiometric YH_{3-x} ($YH_{2.25-2.35}$) resulted from synthesis as judged from the elemental analysis data and X-ray powder diffraction [11]. Anhydrous YCl_3 and YF_3 (99.99%, Sigma Aldrich) were used as received. $NaNH_2BH_3$ and $LiNH_2BH_3$ were synthesized from NH_3BH_3 and NaH (95%, Sigma Aldrich) or $LiNH_2$ (95%, Sigma Aldrich), respectively by disc-milling, according to published procedures [4]. $NaNH_2BH_3$ and $LiNH_2BH_3$ products were tested for purity by XRD powder diffraction, FT-IR measurements (KBr pellets) and elemental combustion analysis [4].

To synthesize $NaNH_2BH_3$ we milled for 3 min NaH and NH_3BH_3 in a molar ratio 1:1 inside a disc mill made of tungsten carbide (Testechem, Poland). $LiNH_2BH_3$ was obtained by milling for 6 min of $LiNH_2$ and NH_3BH_3 in a molar ratio 1:1. Both products were characterized by X-ray powder diffraction (XRD) and their patterns matched well the literature ones [3–5].

Yttrium amidoborane was targeted via five mechanochemical reaction routes, including four methathetic reactions (Eqs. (1)–(4)):

$$YCl_3 + 3LiNH_2BH_3 \rightarrow 3LiCl + Y(NH_2BH_3)_3 \quad (1)$$

☆ Electronic Supplementary Information (ESI) available: FT-IR spectra, XRDPPs, selected TGA/DSC data and results of Elemental Combustion Analysis. See doi:10.1039/b000000x/.

* Corresponding author at: ICM, The University of Warsaw, Pawińskiego 5a, 02106 Warsaw, Poland.
E-mail addresses: rgenova@icm.edu.pl (R.V. Genova), fijalkowski@chem.uw.edu.pl (K.J. Fijalkowski), armand@icm.edu.pl (A. Budzianowski), wg22@cornell.edu (W. Grochala).

0925-8388/$ – see front matter © 2010 Elsevier B.V. All rights reserved.
doi:10.1016/j.jallcom.2010.03.182

$$YCl_3 + 3NaNH_2BH_3 \rightarrow 3NaCl + Y(NH_2BH_3)_3 \quad (2)$$

$$YF_3 + 3NaNH_2BH_3 \rightarrow 3NaF + Y(NH_2BH_3)_3 \quad (3)$$

$$YF_3 + 3LiNH_2BH_3 \rightarrow 3LiF + Y(NH_2BH_3)_3 \quad (4)$$

Mixtures of yttrium halides and alkali metal amidoboranes in a molar ratio 1:3 were milled for 9 min (3 times 3 min with 5 min breaks to avoid overheating). An alternative synthesis, similar to that of alkali amidoboranes (Eq. (5)) [3,4,6], used mixture of YH_{3-x} and NH_3BH_3 in a molar ratio 1:3, milled for 15 min (5 times 3 min, with 5 min breaks):

$$YH_{x\sim3} + 3NH_3BH_3 \rightarrow Y(NH_2BH_3)_3 + 3H_2\uparrow \quad (5)$$

2.2. Wet synthesis

In attempts to obtain a monocrystal of $Y(NH_2BH_3)_3$, wet syntheses were performed in THF (cf. ESI).

2.3. Synthesis of 'thermally decomposed samples'

Batches denoted below as 'thermally decomposed samples' were synthesized in a sealed glass round bottom flask, for as-obtained composites heated to 300 °C at the rate of 10–15 °C min^{-1} in an argon atmosphere. The temperature was monitored with an infrared thermometer (pyrometer). Samples had no contact with air during processing.

2.4. Attempts of separation of $Y(NH_2BH_3)_3$ and LiCl

Attempts of separation of $Y(NH_2BH_3)_3$ from LiCl were performed by dissolving of the as-obtained composite in THF and *t*-butanol (note, LiCl is soluble in these solvents). Unfortunately the solid residue is not crystalline and reflections coming from $Y(NH_2BH_3)_3$ could not be observed). Sublimation attempts failed due to decomposition of $Y(NH_2BH_3)_3$ at high vacuum.

2.5. Instrumentation

Each sample was subject to structural and spectroscopic investigations as well as studies of thermal decomposition. For experimental details (powder X-ray diffraction, FT-IR, TGA/DSC/EGA, elemental combustion analysis), see ESI [6].

2.6. Solid state ^{11}B MAS NMR

Described in detail in ESI. $\delta(Y(NH_2BH_3)_3) = -23.9$ ppm.

3. Results and discussion

3.1. Successful synthesis of $Y(NH_2BH_3)_3$

3.1.1. $YCl_3/LiNH_2BH_3$ composite

Powder X-ray diffraction pattern (XRDP) of the post-reaction composite (Fig. 1) shows peaks originating from LiCl (a presumed by-product of the synthesis according to Eq. (1). Reflections from YCl_3 and $LiNH_3$ cannot be seen suggesting full transformation of substrates into products. Apart from LiCl peaks XRDP contains many strong low angle reflections coming from a new crystalline phase, assumed to be $Y(NH_2BH_3)_3$.

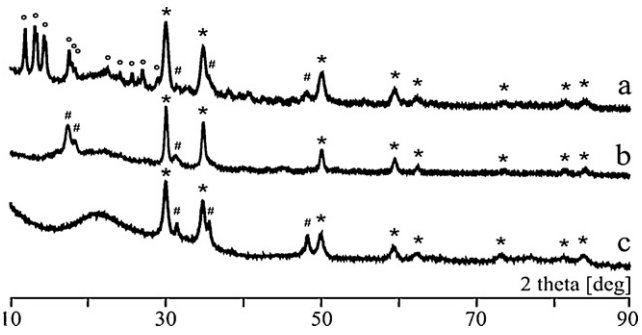

Fig. 1. X-ray powder diffraction data for post-milled $YCl_3/LiNH_2BH_3$ composite (a) at 20 °C; (b) spontaneously decomposed after 4 days in inert gas atmosphere; (c) thermally decomposed at 300 °C. $Y(NH_2BH_3)_3$ (°), LiCl (*) and unidentified phases (#).

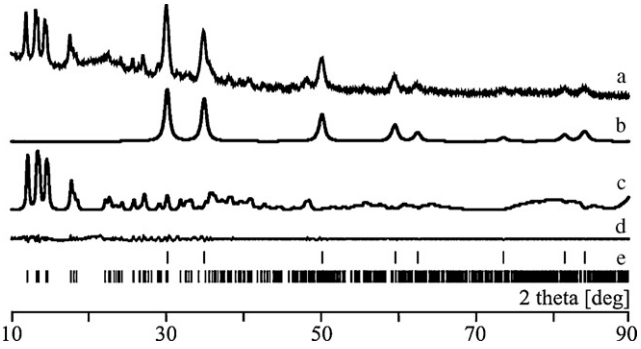

Fig. 2. The Le Bail decomposition of X-ray diffractogram of post-milled $YCl_3/LiNH_2BH_3$ composite (a) $Y(NH_2BH_3)_3$ at 20 °C; (b) calculated curve from LiCl structure refinement; (c) calculated curve of $Y(NH_2BH_3)_3$; (d) difference curve; (e) marks of *h k l* reflections of LiCl (top) and $Y(NH_2BH_3)_3$ (bottom).

The XRDP was indexed using the Le Bail method with simultaneous structure refinement for LiCl [12,13] (Fig. 2). Eventually, the monoclinic cell with unit cell parameters of 13.18902(63) Å, 7.82233(38) Å, 14.874274(68) Å and $\beta = 92.42620(40)°$ in the space group *C*2/*c* (no. 15) has been chosen as a correct solution. The cell volume is 1533.19(13) $Å^3$. Assuming eight formula units (FUs) in the unit cell ($Z = 8$, recall, a general 8f Wyckoff position generates eight equivalent atoms at *C*2/*c* symmetry) one may calculate the volume per formula unit of 191.6 $Å^3$.

An expected volume per FU may be estimated using known molecular volumes of substrates used in the syntheses and a stoichiometric ratio. In one attempt volumes per FU of both substrates were summed, and than volume of LiCl was subtracted; in another one volume of $NH_2BH_3^-$ anion was calculated, tripled and summed with volume of Y^{3+} cation. The obtained values of volume per FU of $Y(NH_2BH_3)_3$ range between 183.4 $Å^3$ and 182.9 $Å^3$, being only ~4% smaller than the one derived from indexation (191.6 $Å^3$). This agreement confirms that the monoclinic *C*2/*c* cell indeed corresponds to $Y(NH_2BH_3)_3$. One might be tempted to fully solve the crystal structure of the title compound; we feel, however, that this would be very difficult without performing additional synchrotron or neutron-scattering measurements.

It seems that LiCl does not incorporate chemically into $Y(NH_2BH_3)_3$ to a considerable degree nor it forms a solid solution; an expected volume per FU of $LiY[Cl(NH_2BH_3)_3]$ falls at 216.6 $Å^3$ and thus it is as much as 18% larger than the expected value.

$Y(NH_2BH_3)_3$ proves to be quite unstable at ambient conditions since its reflections disappear from XRDP when the sample is left for a few days in Ar at room temperature (Fig. 1). We will come back to this important feature below.

Mass loss from $Y(NH_2BH_3)_3$ occurs in the temperature range of 50–300 °C (Fig. 3). Thermal decomposition of the compound seems to be complex, with three weakly exothermic signals present in the DCS profile. Exothermicity of the thermal decomposition suggests that $Y(NH_2BH_3)_3$ is thermodynamically unstable at room temperature due to both enthalpic and entropic contributions to the free Gibbs energy. Thermal decomposition is certainly irreversible because standard free Gibbs energy of the decomposition process is negative. Therefore $Y(NH_2BH_3)_3$ is no different from other metal amidoboranes, all of which decompose exothermally [2–7].

Total mass loss up to 300 °C is 5.5% and it is 10% larger than the theoretical hydrogen content of the composite (4.9%). Qualitative analysis of the gases evolved show that hydrogen is contaminated indeed with significant amount of ammonia in the entire temperature range studied. Evolution of hydrogen polluted with NH_3 was recently observed for sodium amidoborane [6]. Presence of ammonia in the hydrogen evolved is obviously undesirable for low-temperature fuel cell applications.

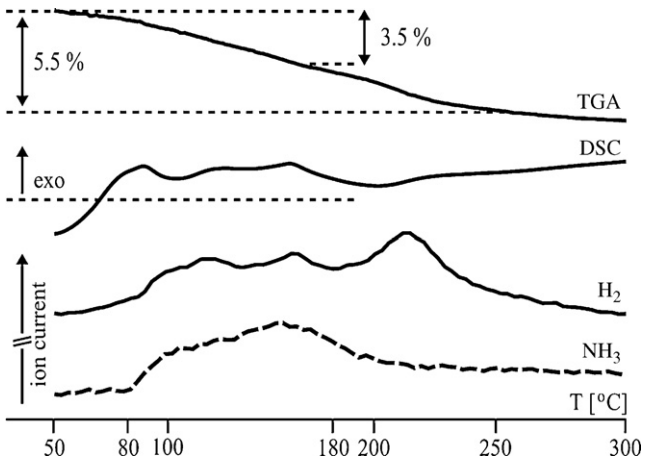

Fig. 3. Thermal decomposition of post-milled $YCl_3/LiNH_2BH_3$ composite at 10 K min^{-1}: TGA and DSC profiles (top), H_2 and NH_3 ion currents (bottom).

The FT-IR spectrum of the post-milled composite consists of several strong absorption bands in the NH and BH stretching and bending regions (Fig. 4). The strongest ν(NH) band (3387 cm^{-1}) is blue-shifted by 27 cm^{-1} while the strongest ν(BH) band (2341 cm^{-1}) by 13 cm^{-1} as compared to analogous bands for $LiNH_2BH_3$. Simultaneously, the lowest frequency ν(BH) bands detected for $Y(NH_2BH_3)_3$ (1908 cm^{-1}, 1951 cm^{-1} and 2098 cm^{-1}) are substantially red-shifted (by 100–125 cm^{-1}) as compared to those measured for $LiNH_2BH_3$. These results suggest that terminal NH and BH bonds of $Y(NH_2BH_3)_3$ are slightly stronger while the bridging BH···M^{n+} bonds are substantially weaker than their counterparts for $LiNH_2BH_3$ (cf. ESI). This kind of interaction should indeed be much stronger for $Y(NH_2BH_3)_3$ than for $LiNH_2BH_3$ due to (i) a larger charge density of Y^{3+} in comparison with Li^+ and (ii) a tendency of transition metals to form strong chemical bonding to boron, which is not preeminent for alkali metals [14].

Interestingly, the strongest ν(NH) band (3387 cm^{-1}) is appreciably red-shifted (by 76 cm^{-1}) as compared to pristine AB. This suggests that a dihydrogen bond interaction [15] of NH_2 group of one amidoborane anion with BH_3 group of adjacent anion is much weaker for $Y(NH_2BH_3)_3$ than for NH_3BH_3.

The IR spectrum of the thermally decomposed composite (Fig. 4) shows very weak ν(NH) and ν(BH) bands while ν(BN) band is very broad and in a wave number range typical for extended BN networks [16,17]. This means majority of hydrogen is released from the

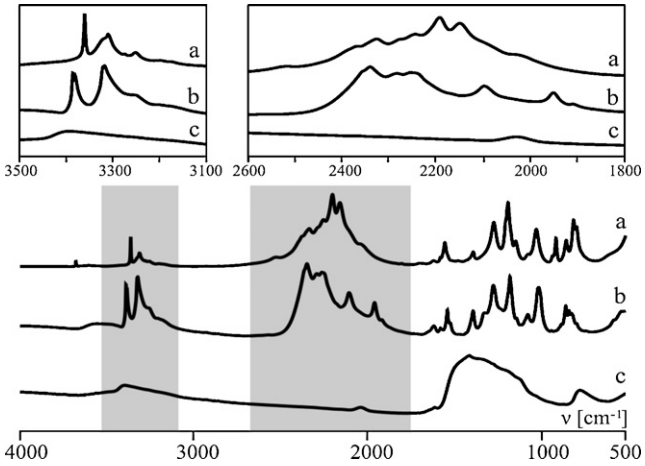

Fig. 4. Bottom: FT-IR spectra for (a) mixture of the substrates; and for post-milled $YCl_3/LiNH_2BH_3$ composite (b) at 20 °C; (c) decomposed at 300 °C. Top: Focus on BH and NH stretching regions.

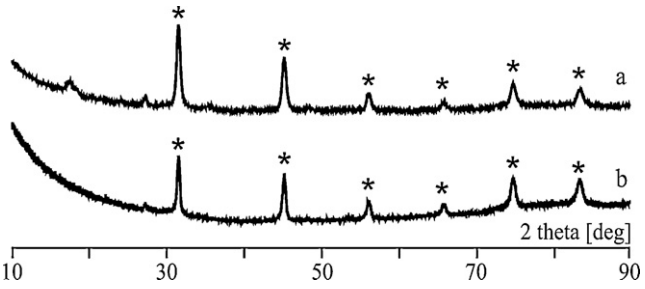

Fig. 5. X-ray powder diffraction data for post-milled $YCl_3/NaNH_2BH_3$ composite (a) at 20 °C; (b) thermally decomposed at 300 °C. Peaks from NaCl are marked with an asterisk (*).

sample during its thermal decomposition. This observation corroborates the observed hydrogen evolution (EGA) and is also consistent with the results of elemental composition analysis (ESI). Chemical nature of decomposition products in the solid state (Y borides? nitrides? etc.) is obviously of interest. Unfortunately, $Y(NH_2BH_3)_3$ heated to 300 °C and cooled to room temperature yields only reflections coming from LiCl by-product and three unassigned peaks (Fig. 1). Thus, most of the product(s) of the thermal decomposition is(are) amorphous.

3.2. $YCl_3/NaNH_2BH_3$ composite

Having successfully synthesized $Y(NH_2BH_3)_3$ using $YCl_3/LiNH_2BH_3$ substrates we have then turned to analogous sodium amidoborane system. The obtained $YCl_3/NaNH_2BH_3$ composite is an off-white powder. Powder XRDPs of the composite and of the product of its thermal decomposition at 300 °C, are shown in Fig. 5. The diffractograms show only NaCl reflections and no reflections from YCl_3 and $NaNH_2BH_3$ substrates thus indicating full conversion to products (Eq. (2)). The methathetic reaction thus proceeds in a similar manner as the one for lithium analogue, but the product obtained is either unstable (and it decomposes during milling) or simply amorphous. Since the FT-IR spectra of the freshly obtained composite (ESI) are very different from those of those measured for its lithium analogue, the first possibility seems more likely.

Mass loss from the $YCl_3/NaNH_2BH_3$ composite takes place in the temperature range of 95–250 °C in one broad step (Fig. 6). Total mass loss of 3% is smaller than hydrogen content of the composite (4.2%). Infrared and mass spectroscopy analyses of the gas released during thermal decomposition show evolution of hydrogen con-

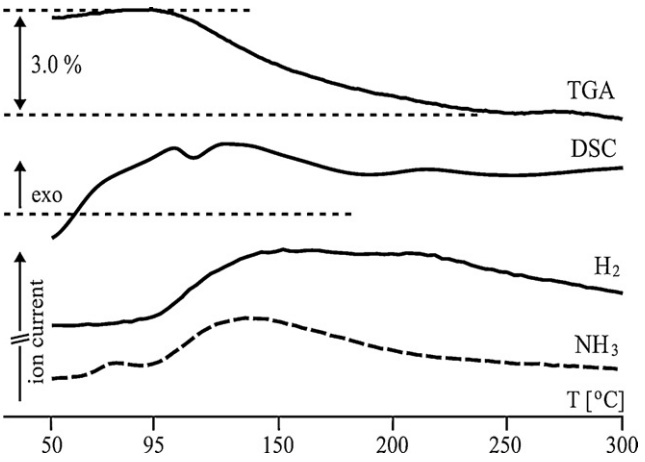

Fig. 6. Thermal decomposition of $YCl_3/NaNH_2BH_3$ at 10 K min^{-1}: TGA and DSC profile (top); H_2 (m/z = 2) and NH_3 (m/z = 17) ion current (bottom).

taminated not only with NH_3 ($m/z = 17$), but also with NH_2BH_3 ($m/z = 30$) and borazine ($m/z = 81$), rendering this composite inferior to its lithium analogue. Thermal decomposition during heating up to 300 °C does not result in formation of any novel crystalline (intermediate or product) phase (Fig. 5).

Thermal decomposition of the composite affects its FT-IR spectrum (ESI). The ν(NH) bands become very weak as compared with the spectrum of the freshly prepared composite. The ν(BH) and ν(BN) bands do not lose their intensity, but they blue-shift suggesting NH_3 evolution without concomitant H loss from BH_3 group; the result is unexpected and it suggests that the pathway of thermal decomposition of the $YCl_3/NaNH_2BH_3$ system is markedly different from that for its lithium analogue.

3.3. $YF_3/NaNH_2BH_3$ composite

Powder XRDPs of the freshly prepared $YF_3/NaNH_2BH_3$ composite is shown in Fig. 7. The post-milled composite contains large amount of the YF_3 substrate but not the expected NaF by-product. Reflections from the second substrate ($NaNH_2BH_3$) cannot be seen, either, probably due to its amorphization during high-energy milling. These results suggest that the mechanochemical reaction described by Eq. (3) did not occur to appreciable extent. Indeed, the FT-IR spectrum of the post-milled composite is very similar to the spectrum of a mixture of the substrates (ESI). The $YF_3/NaNH_2BH_3$ composite must be considered as a plain mixture of homogenized small-grain YF_3 and $NaNH_2BH_3$ rather than the product of a chemical reaction. It is, however, still of interest to what extent the presence of YF_3 affects the thermal decomposition of amorphous $NaNH_2BH_3$.

Thermal decomposition is preceded by an endothermic event at 80 °C (ESI) corresponding to melting of a sample; this is not unexpected since one of the constituents of the composite, $NaNH_2BH_3$, indeed melts around 80–90 °C [6]. Thermal decomposition proceeds in the temperature range of 70–230 °C via a two-step process (ESI). The first one (70–100 °C) leads to a 3.5% mass loss, the second one (100–250 °C) to a 1.0% mass loss. Total mass loss of 4.5% is smaller than the theoretical hydrogen content of the composite (4.9%). Infrared and mass spectroscopic analyses of the evolved gases confirm evolution of H_2 significantly contaminated with both NH_3 and NH_2BH_3.

Strong reflections from YF_3 substrate are still present in the XRDP of the composite heated to 300 °C, together with several new broad signals from NaF and from as yet unknown phase(s) (Fig. 7). However, none of the peaks corresponds to those for $Y(NH_2BH_3)_3$. The thermally activated reaction between $NaNH_2BH_3$ and YF_3 thus seems to proceed to some extent at elevated temperatures but its pathway is different than initially assumed (Eq. (3)).

Thermally decomposed composite gives FT-IR spectrum almost free from ν(NH) bands (ESI). The ν(BH) bands are weaker and red-shifted while the ν(BN) band is broadened and red-shifted.

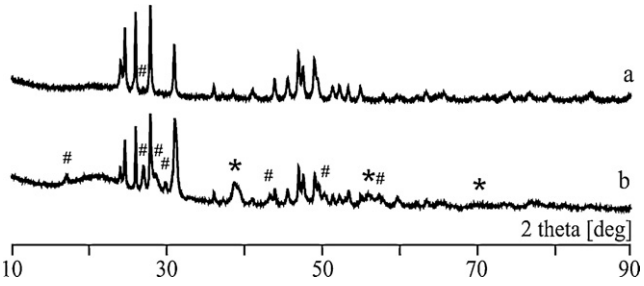

Fig. 7. X-ray powder diffraction data for post-milled $YF_3/NaNH_2BH_3$ composite (a) at 20 °C; (b) thermally decomposed at 300 °C. NaF (*) all unidentified phases (#). Unmarked peaks belong to YF_3.

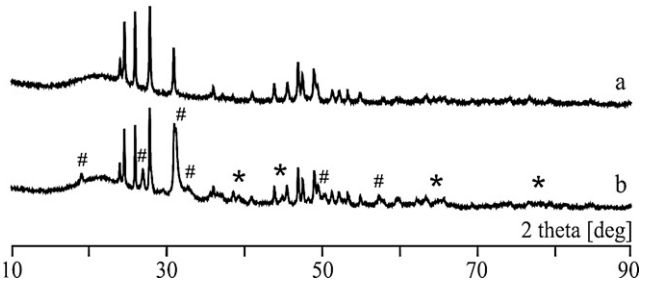

Fig. 8. X-ray powder diffraction data for post-milled $YF_3/LiNH_2BH_3$ composite (a) at 20 °C, just peaks from YF_3; (b) thermally decomposed at 300 °C. LiF (*) and unidentified phases (#).

Decrease of intensity in NH region corresponds to observed H_2 and NH_3 evolution during thermal decomposition.

3.4. $YF_3/LiNH_2BH_3$ composite

Powder XRDPs for the freshly prepared $YF_3/LiNH_2BH_3$ composite is shown in Fig. 8. YF_3 substrate is present in large amount, while reflections from the second substrate ($LiNH_2BH_3$, probably amorphous due to high-energy milling) and from the expected LiF by-product cannot be detected (cf. Eq. (4)). The $YF_3/LiNH_2BH_3$ system thus behaves very similarly to its sodium analogue exhibiting no appreciable degree of a mechanochemical reaction. Indeed, the FT-IR spectra of the post-milled composite and a mixture of substrates, are almost identical (ESI).

Thermal decomposition of the mechanochemically homogenized $YF_3/LiNH_2BH_3$ mixture occurs in the temperature range of 60–250 °C in two exothermic steps (ESI). The first step (60–120 °C) results in a 2% of mass loss, the second step (140–250 °C) in a 4% mass loss. Total observed mass loss of 6% is close to the total theoretical hydrogen content of the composite (5.9%). Spectroscopic analyses of the gases evolved during thermal decomposition (ESI) show that hydrogen is polluted with NH_3 only during the first step of decomposition (60–110 °C). Interestingly, hydrogen evolved during the second step of decomposition (140–250 °C) seems to be very pure since the signals from ammonia are undetectable in the FT-IR and MS spectra of the evolved gases. This feature represents an advantage over other amidoborane systems, since their thermal decomposition is usually associated by emission of NH_3.

XRDP of the composite subjected to thermal decomposition at 300 °C still consists of many strong YF_3 reflections, but peaks coming from LiF and from as yet unidentified phase(s) (different from $Y(NH_2BH_3)_3$) can also be detected (Fig. 8). This suggests that a methathetic process may be thermally activated to a certain extent, just like for the analogous sodium system. In addition, huge drop of intensities of the ν(NH) and ν(BH) bands is observed in the FT-IR spectrum of the composite heated to 300 °C (ESI). These observations are consistent with the partial thermal decomposition of the $YF_3/LiNH_2BH_3$ mixture (as seen in TGA measurements) and they reconfirm the evolution of H_2 and NH_3, as observed in simultaneous EGA studies.

3.5. $YH_{x\sim3}/NH_3BH_3$ composite

Having synthesized yttrium amidoborane via a methathetic reaction (Eq. (1)), we have investigated an alternative synthetic route using stoichiometric mixture of YH_{3-x} and NH_3BH_3 (Eq. (5)), analogous to the one described previously for alkali and alkali earth metal amidoboranes (Eq. (5)) [3,4,6]. Unfortunately, it turned out that the expected reactions does not take to a noticeable degree. This failure is interesting because it suggests that hydride anions bound to a very strong Lewis acid (Y^{3+}) do not have sufficient basic-

ity to undergo coupling with acidic protons from the NH_3 group of AB.

Moreover, hydrogen storage properties of the so-prepared composite are inferior to those for pristine AB since YH_3 introduces a dead mass leading to a decrease of an active H content. Simultaneously, no improvement is seen of other important factors such as onset temperature of thermal decomposition, exothermicity of the decomposition reaction (vide: reversibility) or purity of the evolved H_2 gas (cf. ESI). Last but not least, YH_{3-x} seems not to serve as a catalyst of thermal decomposition of AB (ESI).

4. Conclusions

Crystalline yttrium amidoborane, $Y(NH_2BH_3)_3$, was successfully synthesized for the first time via a methathetic (ligand-exchange) dry mechanochemical reaction between YCl_3 and a stoichiometric amount of $LiNH_2BH_3$. The title compound is an off-white hygroscopic crystalline power, which reacts vigorously (albeit not explosively) with liquid water. Crystallographic unit cell of $Y(NH_2BH_3)_3$, obtained from powder X-ray diffraction data, is C-centered monoclinic ($C2/c$) and contains eight FUs ($Z = 8$). Infrared spectroscopy suggests that a considerable interaction takes place between BH_3 groups and Y^{3+}, leading to a marked lowering of the bridging ν(BH) stretching frequency in comparison with $LiNH_2BH_3$. Simultaneously, a dihydrogen bond interaction between the NH_2 group of one amidoborane anion and the BH_3 group of adjacent anion is much weaker for $Y(NH_2BH_3)_3$ than for NH_3BH_3, and typical for metal amidoboranes.

Yttrium amidoborane was obtained in this work in a homogenous mixture with LiCl. The effective hydrogen capacity of this composite material is 4.9 wt.% as compared to 8.4 wt.% for a hypothetical pure $Y(NH_2BH_3)_3$ phase. Attempts of separation of $Y(NH_2BH_3)_3$ from LiCl by dissolving of the as-obtained composite in THF and *t*-butanol, were unsuccessful, leading unexpectedly to NH_4Cl (cf. ESI). Therefore, hydrogen storage properties of the as-prepared $Y(NH_2BH_3)_3$ were investigated without its separation from the LiCl by-product.

$Y(NH_2BH_3)_3$ is thermodynamically unstable at ambient conditions and it spontaneously decomposes within a few days. A freshly prepared product decomposes in an exothermic ('irreversible') process upon heating (50–250 °C) in argon gas, with concomitant evolution of large amounts of H_2 and of a noticeable ammonia impurity.

Other methathetical reactions tested (using either YF_3 instead of YCl_3, or $NaNH_2BH_3$ instead of $LiNH_2BH_3$, or $YH_{x\sim3}$ and NH_3BH_3) were much less successful, leading either to amorphous products or yielding no ligand exchange at all. One interesting observation is that the $YF_3/LiNH_2BH_3$ composite releases 4 wt.% of pure hydrogen for temperatures over 130 °C.

$Y(NH_2BH_3)_3$ is not a ready-to-use system for storing hydrogen fuel for automotive use, and it requires further chemical modifications before it could be applied in practice. However, successful synthesis of $Y(NH_2BH_3)_3$ is encouraging in context of possible future attempts of synthesis of related amidoboranes of other trivalent metals (Sc, Al, Ga etc.).

Acknowledgements

This research was funded from Marie Curie RTN Hydrogen, EU 6th FP (MRTNCT-2006-032474) and from the SPB grant (37/6PR UE/2007/7) of the Polish Ministry of Science and Higher Education. Authors like to thank Piotr Leszczyński Ph.D., Andrew Churchard, M.Res., and the rest of LTNFM staff for their help in the measurements and fruitful discussions.

Appendix A. Supplementary data

Supplementary data associated with this article can be found, in the online version, at doi:10.1016/j.jallcom.2010.03.182.

References

[1] H.I. Schlesinger, A.B. Burg, J. Am. Chem. Soc. 60 (1938) 290.
[2] W. Grochala, P.P. Edwards, Chem. Rev. 104 (2004) 1283.
[3] Z. Xiong, C.K. Yong, G. Wu, P. Chen, W. Shaw, A. Karkamkar, T. Autrey, M.O. Jones, S.R. Johnson, P.P. Edwards, W.I.F. David, Nat. Mater. 7 (2008) 138.
[4] Z. Xiong, G. Wu, Y.S. Chua, J. Hu, T. He, W. Xu, P. Chen, Energy Environ. Sci. 1 (2008) 360.
[5] H. Wu, W. Zhou, T. Yildirim, J. Am. Chem. Soc. 130 (2008) 14834.
[6] K.J. Fijalkowski, W. Grochala, J. Mater. Chem. 19 (2009) 2043.
[7] H.V.K. Diyabalanage, R.P. Shrestha, T.A. Semelsberger, B.L. Scott, M.E. Bowden, B.L. Davis, A.K. Burrell, Angew. Chem. Int. Ed. 46 (2007) 8995.
[8] Q. Zhang, Ch. Tang, Ch. Fang, F. Fang, D. Sun, L. Ouyang, M. Zhu, J. Phys. Chem. C 114 (2010) 1709.
[9] One might also target scandium amidoborane, $Sc(NH_2BH_3)_3$ with its large theoretical hydrogen content of 11.1 wt.%, but scandium is too expensive for a large-scale commercial use.
[10] Recently hydrogen storage properties of other yttrium containing compounds were thoroughly investigated: T. Sato, K. Miwa, Y. Nakamori, K. Ohoyama, H.W. Li, T. Noritake, M. Aoki, S. Towata, S. Orimo, Phys. Rev. B 77 (2008) 104114; T. Jaroń, W. Grochala, Dalton Trans. (2010) 160.
[11] Y. Wang, M.Y. Chou, Phys. Rev. B 51 (1995) 7500.
[12] R.W.G. Wyckoff, Crystal Structures, vol. 1, second ed., Interscience Publishers, New York, 1963, pp. 85–237.
[13] A.F. Levin'sh, M.E. Straumanis, K. Karlsons, Z. Phys. Chem. Abt. B 40 (1938) 146.
[14] The BN stretching band does not change its wave number appreciably upon formation of $Y(NH_2BH_3)_3$ (ESI).
[15] (a) R. Custelcean, Z.A. Dreger, J. Phys. Chem. B 107 (2003) 9231; (b) R. Custelcean, J.E. Jackson, Chem. Rev. 101 (2001) 1963.
[16] M. Li, L. Xu, L. Yang, Z. Bai, Y. Qian, Diamond Relat. Mater. 18 (2009) 1421.
[17] X. Hao, Y. Wu, J. Zhan, X. Xu, M. Jiang, Cryst. Res. Technol. 40 (2005) 654.